

An *in silico* molecular analysis of the antifungal properties of *Ageratum conyzoides*

Shreyas Sathish¹, Deena Vardhini¹

¹Okinawa Christian School International, Yomitan, Okinawa, Japan

SUMMARY

Fungal infection in crops caused by *Fusarium* species pose serious threats to food security and agricultural productivity, driving the need for effective and selective antifungal agents. One promising candidate is precocene II, a plant-derived compound from *Ageratum conyzoides*, which has been reported to exhibit antifungal properties. However, little is known about the precise molecular mechanism by which precocene II exerts its antifungal effects, particularly against enzymes involved in fungal self-protection. In this study, we investigated the intermolecular interactions between precocene II and trichothecene 3-O-acetyltransferase (Tri101), an enzyme used by *Fusarium* fungi to detoxify their own mycotoxins. We used molecular docking simulations through SwissDock and visualized ligand–protein interactions using the Python Molecular Graphics System (PyMOL) to analyze five top binding positions based on predicted binding affinity. Four out of five simulated positions showed hydrogen bonding interactions involving tyrosine and arginine residues near the enzyme's active site. These findings suggest that precocene II may inhibit Tri101 by binding to catalytically important residues, potentially interfering with the fungus's ability to neutralize its own toxins. This supports the antifungal potential of *A. conyzoides* and lays the groundwork for future design of targeted antifungal compounds.

INTRODUCTION

Fungal infections in crops, particularly those caused by *Fusarium* species, pose a significant global threat to food security and agricultural productivity. These pathogens are responsible for substantial yield losses and the contamination of grains with harmful mycotoxins, impacting both economic stability and public health (1). Addressing these infections is challenging due to the limited availability of selective and environmentally safe antifungal agents (2).

Ageratum conyzoides, commonly known as billygoat weed, is an invasive plant species found in diverse environments worldwide. Its ecological success is largely due to its ability to outcompete native vegetation in both cultivated and disturbed areas (3). This species has drawn scientific interest for its bioactive properties, including antibacterial, insecticidal, and particularly antifungal activity (4). For example, in natural ecosystems, *A. conyzoides* has been observed to inhibit the growth of phytopathogenic fungi, including various *Fusarium* species (5). This antifungal effect is primarily attributed to a secondary metabolite called precocene II, which interferes

with fungal mycelial growth, a process essential for nutrient acquisition and colonization (6).

Previous studies have shown that inhibition of trichothecene 3-O-acetyltransferase (Tri101) can disrupt *Fusarium* species' ability to detoxify their own trichothecene mycotoxins, thereby reducing fungal viability (7, 8). While the antifungal effects of *A. conyzoides* and its secondary metabolite precocene II have been documented, little is known about how precocene II interacts with Tri101 at the molecular level. Ligand–protein complexes are typically stabilized through a combination of noncovalent interactions, including hydrogen bonds, hydrophobic contacts, and π – π stacking, all of which contribute to the specificity and strength of binding (9). *In silico* molecular docking studies provide a way to predict these interactions by generating models of ligand binding conformations, ranked by binding affinity. For enzymes such as Tri101, models that place ligands near catalytically important residues, particularly those capable of forming hydrogen bonds, are considered especially relevant for predicting inhibitory potential (10). Building on this rationale, we sought to explore whether precocene II could form stable, energetically favorable complexes with Tri101 that might block its enzymatic activity.

In this study, we investigated the intermolecular interactions between precocene II and Tri101, an enzyme that enables *Fusarium* species to withstand the toxic effects of their own mycotoxins. We used SwissDock, an online docking platform powered by AutoDock Vina engine, to predict binding affinities (11, 12). We visualized those interactions in three dimensions using PyMOL (Python Molecular Graphics System) a molecular graphics system (13). Unlike traditional experimental methods such as X-ray crystallography, which require the successful expression, purification, and often labor-intensive crystallization of target proteins before structural analysis can even begin, *in silico* techniques provide a more accessible and cost-effective alternative. Obtaining high-quality protein crystals is frequently a major bottleneck, as many proteins fail to crystallize or require extensive optimization over weeks to months. Computational approaches such as molecular docking and molecular dynamics simulations circumvent these experimental constraints, enabling rapid exploration of protein–ligand interactions at atomic-level resolution.

We hypothesized that molecular dynamics simulations of the five highest-ranked docking poses of precocene II bound to Tri101, selected based on predicted binding free energies would reveal at least one conserved hydrogen bond involving shared amino acid residues across multiple poses. These top-ranked docking poses were selected from the docking output based on binding affinity scores. Molecular docking is a computational technique that predicts the preferred orientation of a ligand within a protein's binding site and

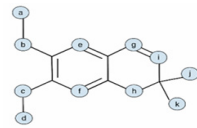
Key:		
Hydrogen Bond: -		
Hydrophobic Contact: -		
Model	Calculated Affinity ΔG (kcal/mol)	Bonds
1	-5.914	h - [TYR]475:A.OH h - [GOL]524:A.O3 - [ARG]479:A.NH2 g [TYR]51:A.CD1 j [TYR]51:A.CE1 k [ALA]477:A.CB i [VAL]469:A.CG1
2	-5.730	b - [TYR]475:A.OH c - [TYR]475:A.OH j [GLN]358:A.CG k [VAL]40:A.CG1 i [ALA]36:A.CB g [ILE]39:A.CD1
3	-5.575	f [TYR]51:A.CE1 h - [TYR]475:A.OH k [VAL]469:A.CG1 g [LEU]435:A.CD2 i [ILE]437:A.CD1
4	-5.463	j [HIS]414:A.CD2 g [TYR]51:A.CE1 h - [GOL]524:A.O3 - [ARG]479:A.NH2
5	-5.405	e [LEU]435:A.CD2 f [TYR]51:A.CE1 k [ILE]39:A.CD1

Table 1. Calculated binding free energies (ΔG , kcal/mol) and observed ligand–protein contacts for the five most favorable docking models of precocene II with trichothecene 3-O-acetyltransferase (PDB ID: 3FOT). Docking was performed using SwissDock with AutoDock Vina scoring. Reported ΔG (kcal/mol) values are those generated by SwissDock. Ligand–protein contacts are presented using standard structural notation, with residue name, residue number, chain identifier, and interacting atom specified. Intermolecular contacts are indicated by a dash between interacting atoms. Hydrogen bonds were identified using PyMOL, and non-polar contacts within 5 Å are included. Each docking model corresponds to one in silico docking pose. Each point on the precocene II ligand corresponds with a lowercase letter as shown in the key.

estimates the strength of binding. Binding affinity scores are commonly used in protein–ligand docking studies to prioritize biologically relevant interaction modes (14). Given the role of hydrogen bonding in stabilizing ligand–protein complexes, these residues may represent key points of interaction. If confirmed by experimental studies, our findings could guide the development of selective antifungal agents derived from *A. conyzooides* that target Tri101 and impair fungal self-defense mechanisms.

RESULTS

We hypothesized that precocene II would bind to Tri101 in positions that include at least one hydrogen bond with amino acid residues common across top-ranked docking models. To test this, we performed molecular docking simulations using SwissDock and analyzed the five top-ranked ligand-binding models based on predicted binding affinity (11). The protein structure used in this study was obtained from the Protein Data Bank (PDB ID: 3FOT), representing the enzyme from *Fusarium sporotrichioides* (15). These five positions were selected because they had the most negative Gibbs free energy (ΔG) values, indicating the strongest and most energetically favorable predicted interactions (16). We visualized these interactions using PyMOL.

For each of these docking model positions, we examined the amino acid residues located within a 5 Å radius of precocene II, a commonly used cutoff distance in molecular docking analyses to identify residues likely to participate in direct or water-mediated interactions with the ligand (16). This threshold captures most hydrogen bonding and significant van der Waals contacts without including residues too far from the ligand to contribute meaningfully to binding. We identified the residues within this radius that were involved in hydrogen bonding interactions and determined the estimated binding affinities and corresponding hydrogen bond contacts (**Table 1**). Our computational analysis identified five potential binding sites on the surface of the enzyme. Among these, residues Tyr475 and Arg479 were predicted to form a likely binding region based on docking interactions (**Figure 1**).

In the first model, we observed hydrogen bonds between precocene II and tyrosine 475, as well as between precocene II and arginine 479, with the latter interaction mediated via a glycerol molecule with a calculated affinity of ΔG -5.914 kcal/mol (**Figure 2**). In the second model, we observed two hydrogen bonds with tyrosine 475 with ΔG -5.730 kcal/mol (**Figure 3**). In the third model, we observed a single hydrogen bond with tyrosine 475 with ΔG -5.575 kcal/mol (**Figure 4**). In the fourth model, we observed a hydrogen bond with arginine 479 via glycerol with ΔG -5.463 kcal/mol (**Figure 5**). In the fifth model, we did not detect any hydrogen bond interactions with ΔG -5.405 kcal/mol (**Figure 6**), suggesting that the ligand was oriented away from hydrogen bond donors or acceptors in this conformation.

DISCUSSION

In our study, we investigated whether precocene II could inhibit Tri101 through specific molecular interactions. We hypothesized that the highest-affinity docking models would reveal at least one hydrogen bond with amino acid residues common across different conformations, and our results supported this hypothesis. We observed that precocene II formed hydrogen bonds with tyrosine 475 and arginine 479 in four out of the five top-ranked docking models within Tri101.



Figure 1. Precocene II occupies a shallow surface pocket on trichothecene 3-O-acetyltransferase (PDB 3FOT). The full enzyme is shown as a grey cartoon to provide structural context. All residues that lie within 5 Å of the docked ligand are shown as element-colored sticks (carbon in green, nitrogen in blue, oxygen in red). The ligand, precocene II is rendered in cyan sticks. Yellow dashed lines mark the hydrogen bonds detected in PyMOL between precocene II and the pocket residues that correspond to Tyr 475 and Arg 479 (see **Table 1 for numerical details).**

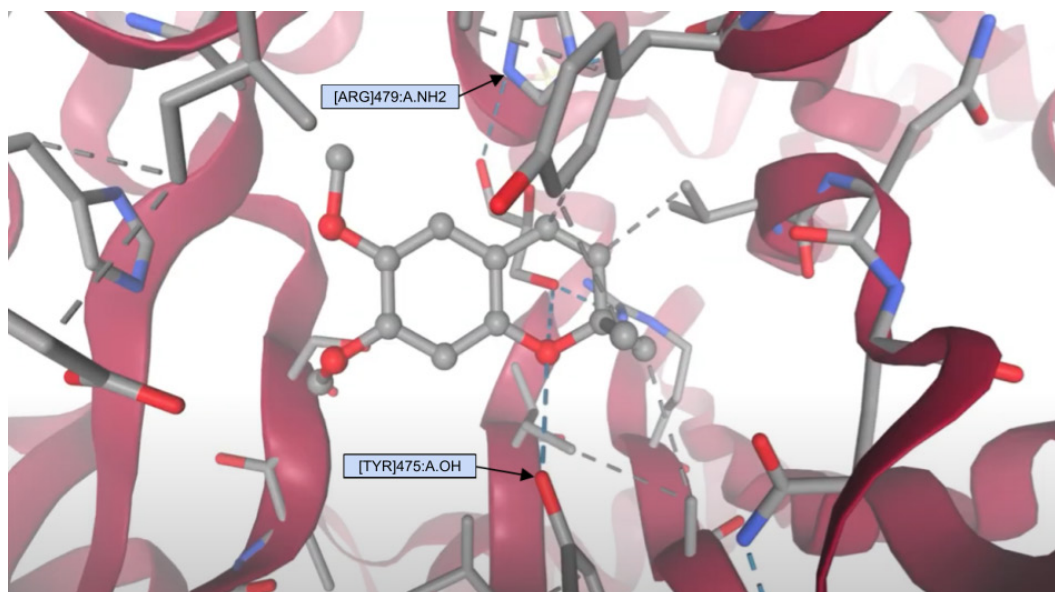


Figure 2. Docking model 1 indicates precocene II forms two hydrogen bonds with Tyr 475 and Arg 479 in trichothecene 3-O-acetyltransferase (PDB 3FOT). The protein backbone is displayed as a pink ribbon, with all side chains within 5 Å of the ligand shown as grey sticks. Precocene II (grey ball-and-stick; carbon in grey, nitrogen in blue, oxygen in red) is positioned in the shallow pocket identified by SwissDock (AutoDock Vina scoring; $\Delta G = -5.914$ kcal/mol, **Table 1**, model 1). Dashed grey lines are non-polar interactions. Dashed blue lines mark hydrogen bonds calculated in PyMOL: 2.8 Å between the ligand carbonyl oxygen and the NH_2 group of Arg 479, and 3.0 Å between the ligand methoxy oxygen and the hydroxyl group of Tyr 475. Distances are annotated next to each bond.

These amino acid residues are often found in protein active or binding sites and play important roles in stabilizing ligand–protein interactions. Tyrosine, with its hydroxyl group, can act as both a hydrogen bond donor and acceptor, while arginine's positively charged guanidinium group supports strong electrostatic and hydrogen-bond interactions with polar or negatively charged ligands (17). Although no previous studies specifically examine these two residues in Tri101, research on related acetyltransferases in other fungal species has shown similar aromatic and positively charged residues to be important for ligand stabilization and catalytic function (18).

These findings indicate that candidate antifungal compounds, especially future derivatives of precocene II, could be intentionally designed to interact with residues such as tyrosine and arginine. Selectivity is key for efficient antifungal effects because antifungal agents that target conserved residues in both pathogenic and non-pathogenic organisms risk off-target effects (19). Designing selective inhibitors often requires exploiting subtle structural differences between homologous enzymes in target versus non-target species. Tri101 is conserved across multiple *Fusarium* species and other trichothecene-producing fungi (20), suggesting that inhibitors designed for this active site could have broad application within this pathogen group.

Although precocene II is widely recognized for its insecticidal effects, several studies have documented its antifungal activity. For instance, it has been reported to inhibit the growth of *Fusarium* species by disrupting mycelial expansion (5). Our findings offer a potential molecular explanation for this effect by suggesting that precocene II may interfere with trichothecene detoxification, a process essential for fungal pathogenicity because unmodified trichothecenes inhibit protein synthesis and reduce fungal viability (21). By directly binding to the active site of Tri101, precocene II could

impair this detoxification pathway and reduce the pathogen's ability to colonize host plants.

The absence of hydrogen bonds in one of the five docking models highlights the variability inherent in protein–ligand interactions. Factors such as ligand orientation, steric hindrance, or suboptimal proximity to donor/acceptor groups can limit hydrogen bond formation (22). In our study, the fifth model placed the ligand in an orientation that positioned key functional groups away from hydrogen bond donors or acceptors, reducing binding stability. Evaluating

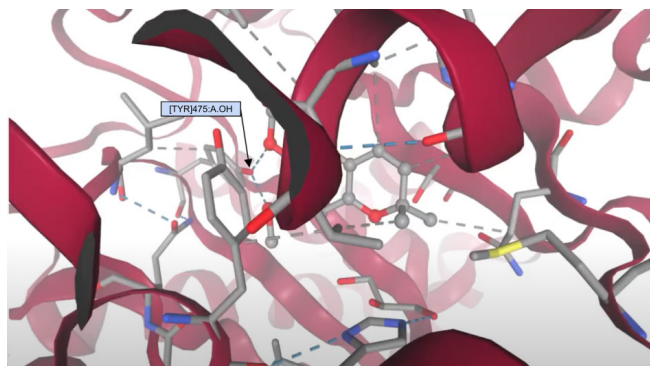


Figure 3. Docking model 2 indicates precocene II engages two hydrogen bonds exclusively with Tyr 475 of trichothecene 3-O-acetyltransferase (PDB 3FOT). The enzyme backbone is shown as a pink ribbon; all side chains within five Å of the ligand are displayed as grey sticks. Precocene II is rendered in grey ball-and-stick (carbon in grey, nitrogen in blue, oxygen in red); dashed blue lines denote hydrogen bonds identified in PyMOL. In this model (SwissDock AutoDock Vina score $\Delta G = -5.730$ kcal/mol, **Table 1**, model 2), the ligand forms a 2.7 Å bond from its methoxy oxygen (upper left) and a 3.0 Å bond from its carbonyl oxygen (lower right) to the hydroxyl group of Tyr 475 (labelled). No contacts with Arg 479 or other residues were observed in this orientation.

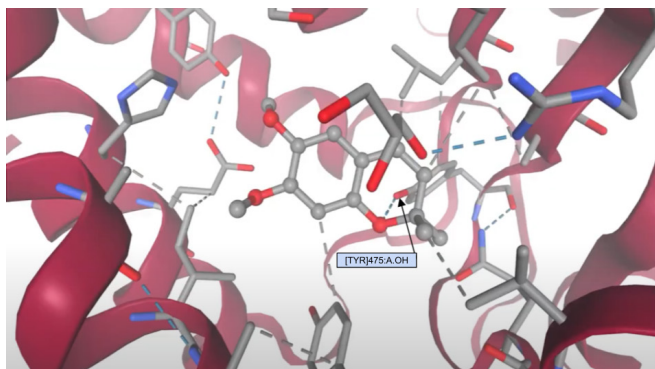


Figure 4. Docking model 3 indicates precocene II forms a single hydrogen bond with Tyr 475 of trichothecene 3-O-acetyltransferase (PDB 3FOT). The protein backbone is shown as a pink ribbon; all side chains within five Å of the ligand are rendered as grey sticks. Precocene II appears in grey ball-and-stick (carbon in grey, nitrogen in blue, oxygen in red). A single hydrogen bond (dashed blue line, 2.9 Å) links the ligand carbonyl oxygen to the hydroxyl group of Tyr 475 (labelled). No contacts with Arg 479 are present in this orientation. This model ranks third among the SwissDock solutions (AutoDock Vina score $\Delta G = -5.575$ kcal/mol. **Table 1**, model 3).

multiple binding models allowed us to identify consistent residue interactions while recognizing these conformational limitations.

One limitation of this study is that we focused on only five of the eighteen models generated by SwissDock, selecting those with the most favorable binding affinities (ΔG). While this approach balances interpretability and computational feasibility, expanding the number of analyzed models in future studies could reveal additional binding motifs and improve statistical reliability. Moreover, *in vitro* validation techniques such as site-directed mutagenesis or enzyme activity assays would be essential to confirm these predicted interactions and assess their functional relevance.

In conclusion, our *in silico* docking analysis suggests that precocene II may inhibit the fungal detoxification enzyme Tri101 through hydrogen bonding with key residues such as tyrosine 475 and arginine 479. These interactions provide a plausible molecular mechanism for the antifungal activity of precocene II against *Fusarium* species and highlight specific contact points that could inform future structure-based drug design. Derivatives of precocene II that enhance binding affinity or selectivity for this fungal enzyme could offer promising leads for the development of eco-friendly, plant-based antifungal agents applicable in both agricultural and medical settings.

MATERIALS AND METHODS

Structure Retrieval

The Simplified Molecular Input Line Entry System (SMILES) is a chemical notation format that digitally represents molecular structures in a way that can be processed by computational tools (23). The SMILES notation for precocene II was obtained from the PubChem database (24). The three-dimensional structure of the target protein, trichothecene 3-O-acetyltransferase (Tri101) from *Fusarium sporotrichioides*, was retrieved from the Protein Data Bank (PDB ID: 3FOT) (15).

Molecular Docking Simulations

Molecular docking simulations were performed using SwissDock, a web-based platform for small-molecule docking (11). SwissDock uses the AutoDock Vina algorithm to predict binding sites and estimate binding affinities. Eighteen potential binding models of precocene II were generated and automatically ranked based on their estimated binding free energies, expressed in kcal/mol. These energy values are reported in **Table 1**. All docking runs were performed using SwissDock default parameters, with no manual adjustments to scoring functions or search space beyond specifying the target protein and ligand.

From the eighteen models, we selected the five with the lowest (most favorable) binding free energies for detailed analysis. This approach is standard in computational docking studies, as it focuses on the most energetically favorable and biologically plausible poses while balancing computational efficiency with structural insight (25, 26).

Visualization

The selected docking conformations were visualized using PyMOL (Python Molecular Graphics System) (13). Prior to visualization, the protein structure was cleaned by removing non-essential molecules such as water and crystallization ligands. Interactions between precocene II and Tri101 were evaluated by identifying amino acid residues located within a five Å radius of the ligand, a commonly used cutoff in docking analyses to capture hydrogen bonding and relevant van der Waals interactions (27). Hydrogen bonding interactions were recorded when the donor–acceptor distance was ≤ 3.5 Å and the donor–hydrogen–acceptor angle was $\geq 120^\circ$, consistent with accepted geometric criteria (28).

Data and Resource Availability

All computational tools used in this study are publicly available. No custom scripts or algorithms were developed or applied during the research process.

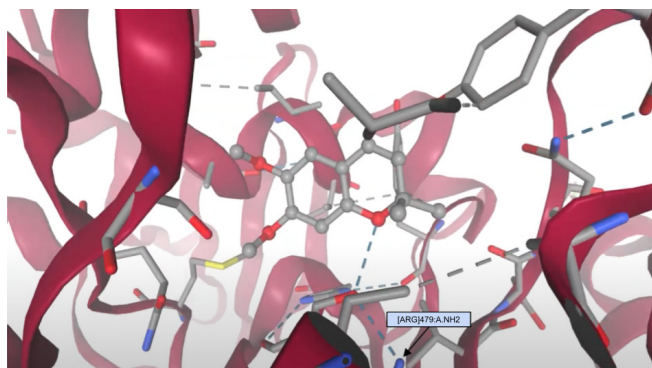


Figure 5. Docking model 4 indicates precocene II hydrogen-bonds with Arg 479 via an interfacial glycerol molecule in trichothecene 3-O-acetyltransferase (PDB 3FOT). The enzyme backbone is illustrated as a pink ribbon; all side-chain atoms within 5 Å of the ligand are displayed as grey sticks. Precocene II is rendered as a grey ball-and-stick model (carbon in grey, nitrogen in blue, oxygen in red), and the crystallographic glycerol is shown as yellow sticks. A hydrogen bond (blue dashed line, 3.1 Å) bridges the ligand carbonyl oxygen to the NH_2 group of Arg 479 (labelled) through the glycerol hydroxyl. No contacts with Tyr 475 are detected in this orientation. This model is the fourth-best SwissDock solution (AutoDock Vina score $\Delta G = -5.463$ kcal/mol. **Table 1**, model 4).

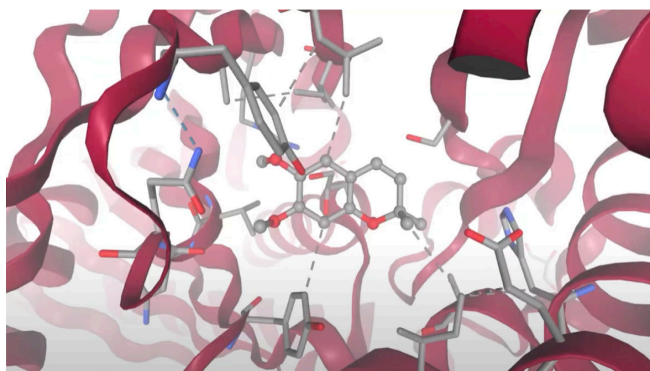


Figure 6. Docking model 5 indicates precocene II binds in an alternative orientation with no hydrogen bonds to nearby residues of trichothecene 3-O-acetyltransferase (PDB 3FOT). The protein backbone is displayed as a pink ribbon, and all side chains within 5 Å of the ligand are rendered as grey sticks. Precocene II is shown in grey ball-and-stick representation (carbon in grey, nitrogen in blue, oxygen in red). Unlike Models 1-4, this SwissDock solution (AutoDock Vina score $\Delta G = -5.405$ kcal/mol. **Table 1**, model 5) places the ligand in a rotated orientation such that no heavy-atom contacts ≤ 3.5 Å are present; consequently, no hydrogen-bonding interactions (blue dashed lines) are detected.

Received: December 27, 2024

Accepted: June 23, 2025

Published: April 28, 2026

REFERENCES

- Johns, L. E., et al. "The Changing Threat of *Fusarium* Head Blight Mycotoxins in European Wheat." *Nature Food*, vol. 3, 2022, pp. 1011–1021. <https://doi.org/10.1038/s43016-022-00655-z>.
- Antonissen, G., et al. "The Impact of *Fusarium* Mycotoxins on Human and Animal Health." *Toxins*, vol. 6, no. 2, 2014, pp. 548–568. <https://doi.org/10.3390/toxins6020430>.
- Kamboj, A., and A. K. Saluja. "Ageratum conyzoides L.: A Review on Its Phytochemical and Pharmacological Profile." *International Journal of Green Pharmacy*, vol. 2, no. 2, 2008, pp. 59–68. <https://www.greenpharmacy.info/index.php/ijgp/article/view/29>.
- Kaur, A., et al. "Ecology, Biology, Environmental Impacts, and Management of an Agro-Environmental Weed *Ageratum conyzoides*." *Plants*, vol. 12, no. 12, 2023, article 2329. <https://doi.org/10.3390/plants12122329>.
- Nur Hazirah, M. F., et al. "Antifungal Activity of *Ageratum conyzoides* Extract against *Fusarium oxysporum* in Musa spp." *IOP Conference Series: Earth and Environmental Science*, vol. 1182, no. 1, 2023, article 012074. <https://doi.org/10.1088/1755-1315/1182/1/012074>.
- Furukawa, T., et al. "Precocene II, a Trichothecene Production Inhibitor, Binds to Voltage-Dependent Anion Channel and Increases the Superoxide Level in Mitochondria of *Fusarium graminearum*." *PLOS ONE*, vol. 10, no. 8, 2015, e0135031. <https://doi.org/10.1371/journal.pone.0135031>.
- Maeda, K., and S. Ohsato. "Molecular Genetic Characterization of *Fusarium graminearum* Genes Identified as Encoding a Precocene II-Binding Protein." *Mycoscience*, vol. 67, no. 1, 2016, pp. 3–8. <https://doi.org/10.2520/myco.67-1-3>.
- Garvey, G. S., et al. "Structural and Functional Characterization of the TRI101 Trichothecene 3-O-Acetyltransferase from *Fusarium sporotrichioides*." *Journal of Biological Chemistry*, vol. 283, no. 25, 2008, pp. 16679–16686. <https://doi.org/10.1074/jbc.M705752200>.
- Ferreira de Freitas R and M. Schapira. A systematic analysis of atomic protein–ligand interactions in the PDB. *Med Chem Commun*. 2017;8(10):1970–1981. <https://doi.org/10.1039/C7MD00381A>.
- Hubbard, R. E., and M. K. Haider. "Hydrogen Bonds in Proteins: Role and Strength." *Encyclopedia of Life Sciences*, 2010. <https://doi.org/10.1002/9780470015902.a0003011.pub2>.
- Bugnon, M., et al. "SwissDock 2024: Major Enhancements for Small-Molecule Docking with Attracting Cavities and AutoDock Vina." *Nucleic Acids Research*, vol. 52, no. W1, 2024, pp. W324–W332. <https://doi.org/10.1093/nar/gkae300>.
- Eberhardt, J., et al. "AutoDock Vina 1.2.0: New Docking Methods, Expanded Force Field, and Python Bindings." *Journal of Chemical Information and Modeling*, vol. 61, no. 8, 2021, pp. 3891–3898. <https://doi.org/10.1021/acs.jcim.1c00203>.
- Schrödinger, LLC. "The PyMOL Molecular Graphics System, Version 3.0." 2024, <https://pymol.org>. Accessed 13 Aug. 2025.
- Trott, O., and A. J. Olson. "AutoDock Vina: Improving the Speed and Accuracy of Docking with a New Scoring Function." *Journal of Computational Chemistry*, vol. 31, no. 2, 2010, pp. 455–461. <https://doi.org/10.1002/jcc.21334>.
- Berman, H. M., et al. "The Protein Data Bank." *Nucleic Acids Research*, vol. 28, no. 1, 2000, pp. 235–242. <https://doi.org/10.1093/nar/28.1.235>.
- Ferreira, L. G., et al. "Molecular Docking and Structure-Based Drug Design Strategies." *Molecules*, vol. 20, no. 7, 2015, pp. 13384–13421. <https://doi.org/10.3390/molecules200713384>.
- Lin, H., and J. Luengo. "Exploiting Binding-Site Arginines in Drug Design: Recent Examples." *Bioorganic & Medicinal Chemistry Letters*, vol. 30, no. 17, 2020, article 127442. <https://doi.org/10.1016/j.bmcl.2020.127442>.
- Vetting, M. W., et al. "Structure and Functions of the GNAT Superfamily of Acetyltransferases." *Archives of Biochemistry and Biophysics*, vol. 433, no. 1, 2005, pp. 212–226. <https://doi.org/10.1016/j.abb.2004.09.003>.
- Perfect, J. R. "The Antifungal Pipeline: A Reality Check." *Nature Reviews Drug Discovery*, vol. 16, no. 9, 2017, pp. 603–616. <https://doi.org/10.1038/nrd.2017.46>.
- Kimura, M., et al. "Features of Tri101, the Trichothecene 3-O-Acetyltransferase Gene, Related to the Self-Defense Mechanism in *Fusarium graminearum*." *Bioscience, Biotechnology, and Biochemistry*, vol. 62, no. 5, 1998, pp. 1033–1036. <https://doi.org/10.1271/bbb.62.1033>.
- McCormick, S. P., et al. "Disruption of TRI101, the Gene Encoding Trichothecene 3-O-Acetyltransferase, Reduces Trichothecene Resistance in *Fusarium graminearum*." *Applied and Environmental Microbiology*, vol. 65, no. 12, 1999, pp. 5252–5256. <https://doi.org/10.1128/AEM.65.12.5252-5256.1999>.
- Sousa, S. F., et al. "Protein–Ligand Docking: Current Status and Future Challenges." *Proteins*, vol. 65, no. 1,

- 2006, pp. 15–26. <https://doi.org/10.1002/prot.21082>.
23. Weininger, D. "SMILES, a Chemical Language and Information System. 1. Introduction to Methodology and Encoding Rules." *Journal of Chemical Information and Computer Sciences*, vol. 28, no. 1, 1988, pp. 31–36. <https://doi.org/10.1021/ci00057a005>.
24. Kim, S., et al. "PubChem Substance and Compound Databases." *Nucleic Acids Research*, vol. 44, no. D1, 2016, pp. D1202–D1213. <https://doi.org/10.1093/nar/gkv951>.
25. Agu, P. C., et al. "Molecular Docking as a Tool for the Discovery of Novel Nutraceutical Bioactivities." *Scientific Reports*, vol. 13, 2023, article 10638. <https://doi.org/10.1038/s41598-023-40160-2>.
26. Paggi, J. M. "The Art and Science of Molecular Docking." *Annual Review of Biochemistry*, vol. 93, 2024, pp. 1–25. <https://doi.org/10.1146/annurev-biochem-030222-120000>.
27. Morris, G. M., et al. "Automated Docking Using a Lamarckian Genetic Algorithm and an Empirical Binding Free Energy Function." *Journal of Computational Chemistry*, vol. 19, no. 14, 1998, pp. 1639–1662. [https://doi.org/10.1002/\(SICI\)1096-987X\(19981115\)19:14<1639::AID-JCC10>3.0.CO;2-B](https://doi.org/10.1002/(SICI)1096-987X(19981115)19:14<1639::AID-JCC10>3.0.CO;2-B).
28. McDonald, I. K., and J. M. Thornton. "Satisfying Hydrogen Bonding Potential in Proteins." *Journal of Molecular Biology*, vol. 238, no. 5, 1994, pp. 777–793. <https://doi.org/10.1006/jmbi.1994.1334>.
29. **Copyright:** © 2026 Sathish and Vardhini. All JEI articles are distributed under the Creative Commons Attribution Noncommercial No Derivatives 4.0 International License. This means that you are free to share, copy, redistribute, remix, transform, or build upon the material for any purpose, provided that you credit the original author and source, include a link to the license, indicate any changes that were made, and make no representation that JEI or the original author(s) endorse you or your use of the work. The full details of the license are available at <https://creativecommons.org/licenses/by-nc-nd/4.0/deed.en>.